Early Visual Deprivation Impairs Functional Development of the Visual Ventral Stream

Yifan Xiang,[1] Jingwen Yang,[2,6] Leyan Gao,[2] Zelin Chen,[3] Jingjing Chen,[1] Zhirui Yang,[4] Xiaoqing Gao,[5] Zhuoling Lin,[1] Xiaohang Wu,[1] Shuo Lu,[2,6] and Haotian Lin[1,7,8]

[1]State Key Laboratory of Ophthalmology, Zhongshan Ophthalmic Center, Sun Yat-Sen University, Guangdong Provincial Key Laboratory of Ophthalmology and Vision Science, Guangdong Provincial Clinical Research Center for Ocular Diseases, Guangzhou, China
[2]Neurolinguistics Laboratory, College of International Studies, Shenzhen University, Shenzhen, China
[3]School of Computer Science and Engineering, Sun Yat-Sen University, Guangzhou, China
[4]Department of Linguistics and Modern Languages, The Chinese University of Hong Kong, Hong Kong
[5]Center for Psychological Sciences, Zhejiang University, Hangzhou, China
[6]Department of Clinical Neurolinguistic Research, Mental and Neurological Diseases Research Center, The Third Affiliated Hospital of Sun Yat-Sen University, Guangzhou, China
[7]Hainan Eye Hospital and Key Laboratory of Ophthalmology, Zhongshan Ophthalmic Center, Sun Yat-Sen University, Haikou, China
[8]Center for Precision Medicine and Department of Genetics and Biomedical Informatics, Zhongshan School of Medicine, Sun Yat-Sen University, Guangzhou, China

Correspondence: Haotian Lin, State Key Laboratory of Ophthalmology, Zhongshan Ophthalmic Center, Sun Yat-Sen University, 7# Jinsui Road, Guangzhou, China;
linht5@mail.sysu.edu.cn.
Shuo Lu, Neurolinguistics Laboratory, College of International Studies, Shenzhen University, 3688# Nanhai Road, Shenzhen, China;
lushuo@szu.edu.cn.

YX, JY, and LG contributed equally to the work presented here and should therefore be regarded as equivalent authors.

PURPOSE. To probe the dynamic alternations of neural networks in real-time visual processing after visual deprivation (VD) removal.

METHODS. A prospective cross-sectional study was conducted. Twenty children with a history of early binocular VD caused by congenital cataracts and 20 matched typically developing (TD) children were enrolled. The event-related potential (ERP) data were obtained via high-density electroencephalography. ERP data were analyzed based on three components (P1, N170, and P2), three test conditions (objects, human faces, and Chinese characters), and peak time and region of interest (ROI) chosen on a grand average head map collapsed from the averaged waveform of each group. Source localization and alpha power spectrum density were applied to define the functional pattern of brain areas and evaluate the attention function.

RESULTS. The VD group showed significantly lower P1 amplitudes than the TD group under all conditions in peak ROIs, which were situated in the left occipito-temporal region. For both VD and TD groups, there were strong N170 effects in the character and human face conditions in the component's peak ROIs. Furthermore, source mapping indicated that the VD group generally showed significantly lower activation in the visual cortex and ventral stream, whereas the beyond network areas (mostly frontal areas) intensively participated in functional compensation in the VD group. The VD group showed significant poststimulus alpha desynchronization in object recognition.

CONCLUSIONS. Our research described the mechanisms of visual networks after early binocular VD removal. Our findings may provide a new basis for the poor visual recovery after early binocular VD removal and offer clues for visual recovery strategies.

Keywords: visual deprivation, visual network, ventral stream, functional pattern, high-density electroencephalography

The visual pathway consists of the eyeball, optic nerve, and visual brain regions, of which the visual cortex is the core.[1–3] Physiologically, visual stimuli are processed by parts of the visual pathway and then recognized by individuals.[4] In some pathological conditions, the binocular structure is damaged or dysfunctional, preventing the processing of visual stimuli, a condition known as *visual deprivation* (VD). VD impairs the normal function of the optic nerve and visual brain regions.[5–9] More than 10 million children worldwide experience innate binocular VD and the subsequent functional abnormality of visual cortex development, which persists and affects visual recovery even after the cause of VD has been removed.[10]

In accordance with increasing realization that successful visual processing recruits not only the visual cortex but also the dorsal and ventral streams involving widespread networks, several previous studies have found that early VD may cause different patterns of deficits in visual networks and related dysfunctions, which may persist even after the cause of VD has been removed, causing disappointing

rehabilitation outcomes. Compared with normal controls, VD patients with innate oculopathy were found to exhibit a reduced sensitivity for perceiving global motion[11,12] and global form,[13,14] and to exhibit abnormalities in the visual processing of face stimuli.[15,16] In some other studies, even after prolonged early VD, children displayed good shape recognition and certain cerebral cortex development,[17,18] although one found that the dorsal stream was more vulnerable to development.[19] These preliminary findings lead us to take notice of the possible inconsistencies in the impairment characteristics of visual pathways after VD removal.

To further explore the neural functional alternations after early binocular VD and to identify the impaired pattern in whole-brain visual networks, we used high-density electroencephalography (HD-EEG) with 128 and 256 channels to examine visual processing in children after early binocular VD removal based on multiple task-related analyses, including event-related potentials (ERPs), functional sourcing and spectral oscillations of the alpha band. In addition, we used three types of visual stimuli, Chinese characters, human faces and objects, which represented a hierarchy of visual processing complexity and neural response patterns.[20–24]

This novel approach helped confirm that the dorsal pathway remained functional while the ventral stream underwent significant functional deficits. The clearly revealed functional deficiency of networks sheds light on why vision recovery is so poor in children who experienced early VD. In addition, we found that bilateral temporal and frontal areas significantly compensated for visual processing, and children had relatively normal bottom-up attention to object stimuli after VD removal, both of which provide valuable clues for promising rehabilitation strategies.

MATERIAL AND METHODS

This study was a prospective study conducted from August 2019 to December 2021. The VD children were enrolled from the Department of Pediatric Eye Disease in Zhongshan Ophthalmic Center (ZOC), and the control group participants were enrolled from the ocular health examination population of ZOC, which was approved by the Institutional Review Board of the ZOC (2020KYPJ095). Figure 1 shows the overall pipeline of our research.

Participants

Twenty participants with innate binocular VD caused by congenital cataracts and 20 healthy typically developing (TD) controls matched for age, handedness, education, and language environment were enrolled. In addition, data from 21 adults were collected as a healthy adult control group. Informed written consent was obtained from the legal guardians of child participants as well as adult participants. The inclusion criteria for all participants were as follows: (1) aged between five and 10 years old for the child groups and between 18 and 30 years old for healthy adults, (2) were right-handed, (3) studied at kindergarten or primary school according to their age for the child groups and studied at universities or colleges according to age for healthy adults, and (4) grew up in a Mandarin environment. The inclusion criteria for the VD children were as follows: (1) diagnosed with binocular congenital cataracts at birth, (2)

dense opacity of the optic axis at diagnosis, (3) underwent surgical treatment, (4) had a clear axis after treatment, (5) had regular follow-up for more than three years, (6) had no postoperative complications, (7) had the latest binocular and monocular best corrected visual acuities (BCVAs) of lower than 0.8 (Snellen acuity), and (8) had normal electroretinogram results. The exclusion criteria for the VD children were as follows: (1) diagnosed with other ophthalmic diseases or (2) diagnosed with a neurological or mental disorder. The inclusion criteria for the healthy controls were as follows: (1) had no history of ophthalmic diseases and (2) had the latest binocular and monocular BCVAs of more than 1.0 (Snellen acuity). The exclusion criteria for the healthy controls were as follows: (1) diagnosed with any ophthalmic disease except mild refractive error or (2) diagnosed with a neurological or mental illness.

Examination of Ocular Structure and Visual Function

For each participant, we recorded BCVA, ocular pressure, anterior photographs and fundus images. Distant VA was examined with a standard logarithmic E chart, and the binocular BCVA and monocular BCVAs of both eyes were recorded according to Snellen acuity. Ocular pressure was tested with a noncontact tonometer (TX-F, Canon, Tokyo, Japan) to exclude participants with high intraocular pressure (>21 mm Hg). Anterior photographs taken with a slit lamp (BX900, HAAG-STRETT, Switzerland) and fundus images captured with a nonmydriatic ultra-widefield camera (OPTOS Daytona, Dunfermline, UK) were assessed to ensure that the ocular structures were normal. Electroretinograms were measured with MonPackONE (Metrovision, Perenchies, France) to ensure the normal function of the fundus.

Experimental Stimuli

According to the classical literature, the stimuli were 90 grayscale pictures of three conditions: (1) Chinese character, (2) human face, and (3) object. Thirty Asian faces were selected as the stimuli for the human face condition, which included males, females, children and adults. All faces were emotionally neutral without obvious facial expressions. To make the faces as natural as possible, hair and facial contours were preserved. Stimuli materials for the character conditions were selected from the "Commonly Used Chinese Characters Table" issued by the State Language Affairs Commission, China. To ensure the representativeness of the character stimuli, the number of strokes of all selected characters was limited to three to 14, and different structures of glyphs were taken into consideration such that characters were represented in similar proportions, including characters with left-and-right structures, up-and-down structures, semisurrounded structures, and a single font. Stimuli for the object condition included common animals, plants, food, daily necessities, etc. All the stimuli were framed within an area of 420×300 pixels (14.8 cm $\times$ 10.6 cm) on a background of a 1920- $\times$ 1080-pixel screen, with gray as the background color (Supplementary Fig. S1A).

Task Procedure

The experimental procedure was programmed with E-Prime 2.0 software. The experimental instructions were first
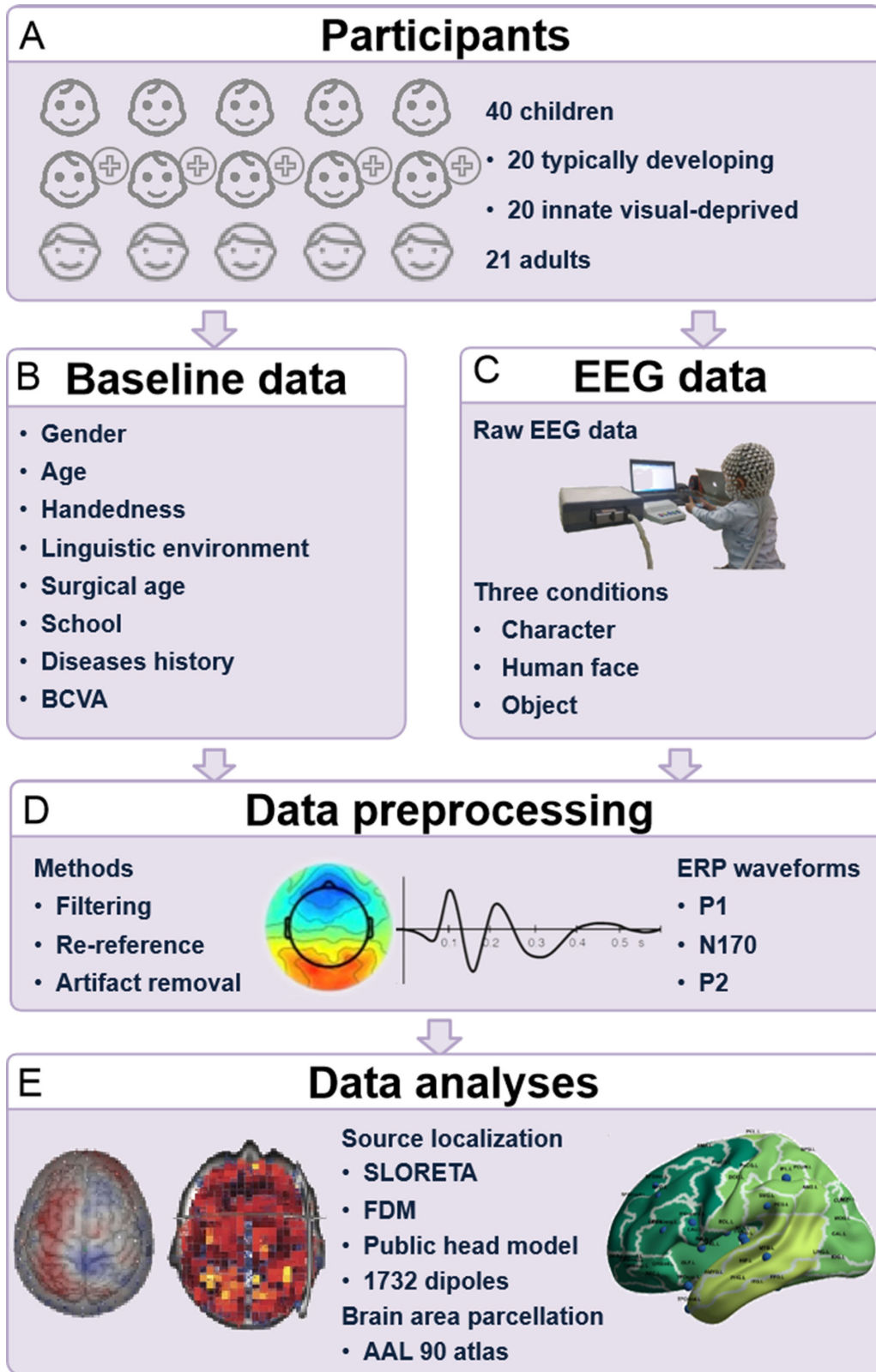
FIGURE 1. The overall pipeline of our research. (**A**) The participants enrolled in our study. (**B**) Collected data at baseline. (**C**) EEG data collected under three conditions. (**D**) Methods for data preprocessing. (**E**) Methods for data analyses. FDM, finite difference method.

presented on the screen, and then the EEG data were collected during a three-minute rest period. Participants were seated in a dimly lit and sound-attenuated room, and no environmental disturbance was allowed to ensure that participants were in a stable condition. Stimuli were presented on a 16-inch DELL monitor (resolution of 1920 × 1080 pixels, 60 p Hz refresh rate) located 80 to 100 cm from participants' eyes with an 11.36° to 14.18° vertical and 20.07° to 24.95° horizontal visual angle for the center. The children were instructed to maintain their attention and finish the passive viewing tasks. Before the task, experimenters followed a protocol to instruct participants to stare at the fixation point on the screen to pay attention to what the pictures referred to during the experiment, and to inform the participants that they would be questioned after the experiment with what was or was not presented. Afterward, the task began, and picture stimuli were randomly presented on the screen for 500 ms. Among each stimulus, there was a random interval of 400 to 600 ms. On account of the young age of child participants and the time required to complete the tasks, the guardians were allowed to accompany their children during the tasks. After the task, experimenters used a list of 10 stimuli to ask every participant about what the pictures referred to and if they had seen them on the screen during the experiment to validate their attention. All participants passed this post-task survey with accuracy rates higher than 75% for the child groups and higher than 95% for the adult group. An example of the task procedure is shown in Supplementary Figures S1B and S1C.

Data Recording

During the experiment, EEG data were recorded with a 128/256-channel Geodesic Sensor Net (Geodesic EEG System 400; Electrical Geodesics Inc., Eugene, OR, USA), referenced online to the vertex (Cz). The number of channels was determined according to the head girth of participants, because 256 channels cannot fit on heads with a girth less than 52 cm. All electrode impedances were kept below 40 kΩ throughout the experiment, and recorded data were sampled at 1000 Hz.

Data Preprocessing

The continuous EEG data obtained in this study were offline filtered (1–30 Hz) and rereferenced to an average reference using the EEGLAB toolbox (Version 2020.0, Delorme and Makeig, 2004), an electrophysiological signal processing toolbox in MATLAB (Version 2018b; MathWorks, Inc., Natick, MA, USA). To improve the signal-to-noise ratio, the Clean Rawdata and ASR tools in EEGLAB were used to exclude artifacts due to head movement, eye blinking, eye movement, and other physiological reasons and more than 80% of trials for each group were retained. Furthermore, independent component analysis with the RUNICA algorithm was conducted to remove artifacts of independent components, including artifacts generated by the subjects (e.g., eye blinks, eye movements and muscle activities) and artifacts induced by recording equipment or testing environment (e.g., line noise). To unify sensor layouts for all participants, interpolation was used to replace missing data. Then the cleaned continuous EEG data were segmented into 700-ms epochs (from −100 to 600 ms rela-

tive to the stimulus onset) and baseline corrected (−100 to 0 ms).

ERP Analysis

After data preprocessing, EEG epochs of each task were then averaged separately in three conditions (character, human face, and object). The key results regarding latency and amplitude of ERPs were measured. For the ERP waveforms, the mean amplitude of each group was calculated over each successive 20-ms time window from 0 to 260 ms after stimulus onset to explore the key ERP components of P1, N170 and P2. Electrodes were grouped into four regions of interest (ROIs): left occipital (O1), right occipital (O2), left temporal-occipital (P7), and right temporal-occipital (P8). The electrode points and corresponding brain regions are clearly distributed in Supplementary Figure S2. In the analysis, ERP waveforms were collapsed across all conditions and participants to create a grand average head map. Then, the ROI waveforms with the highest peak activity were chosen to represent the peak of activity and the approximate time window of each component. The mean activities in these peak ROIs and time windows were then assessed across conditions for further statistical analysis. The amplitudes of N170 and P2 were re-baselined by calculating the peak value difference with P1 considering that their amplitudes were greatly affected by the P1 waves. The component latencies were computed with the fractional area analysis method, which is often superior to peak latency, especially when measured from different waves.[25] This algorithm calculates the area of the waveform above or below the zero line and then defines the time point that divides the area into two areas at 50% as the component latency.

Electrical Source Imaging

Source analysis was conducted through GeoSource 2.0 (Electrical Geodesics Inc., Eugene, OR, USA) with standardized low-resolution electrical tomography algorithms, which have zero localization error in noise-free simulations and are widely used in studies of cognitive and perceptual processing.[26] The standardized low-resolution electrical tomography algorithm is an improved version of its predecessor LORETA that was nevertheless validated for application in similar tasks to the current one.[27] The source imaging of brain activity used a finite difference method realistic head model with 1745 dipoles and the Montreal Neurological Institutes typical head image generated by children aged four to nine years as a template. Source analysis was based on functional brain region parcellations, and automated anatomical labeling (AAL) parcellation with 90 brain regions was adopted.[28] The source localization of scalp EEG at the AAL level has been proven to be reliable by many previous studies.[29–31] Additionally, the dipoles in each brain region were summed to represent the source power of each brain region and further summed into four subnetworks to perform further group and condition comparisons (see details in the section "Task-Activated Source Activities" below). An average filter (with a 20 ms time window size) was also adopted to alleviate some inherent source noise, which exists in most source algorithms. The source imaging and later power spectrum density results were visualized with BrainNet Viewer (http://www.nitrc.org/projects/bnv/).[32]

Alpha Band Power Spectrum Density (PSD)

To evaluate the attention function and top-down/bottom-up attention mediation in visual perception for the VD group, the PSD of the alpha band was computed at each subnetwork summed by AAL regions for two separate epochs: prestimulus alpha power was computed in the period from −500 ms to 0 ms (relative to stimulus presentation), and post-stimulus alpha power was computed from the period 0 ms to 500 ms. The PSD was computed on the respective data segments using the Welch method with a Fast Fourier Transform (FFT) analysis window of 512 time points (1024 ms), with the alpha band range set as 8 to 12 Hz. The FFT window overlap was 500 time points, and a Hamming window was used. Spectral measures were computed by averaging over the stated time and frequency range in the computed spectrogram. The post-stimulus alpha power was re-baselined by subtracting the PSD of the pre-stimulus segment. The PSD was then converted to dB by normalizing the PSD and setting dB = 10*log10 (PSD) (this allows for context in relation to other studies of power).

Statistical Analysis

Statistical analysis was carried out with SPSS 19 (IBM, Armonk, NY, USA). The χ^2 test was used to compare the classified variables of sex and school type, and a nonparametric test and independent-samples T test were used to compare nonnormally distributed variables (binocular and monocular BCVAs) and normally distributed variables (age) between the VD and TD groups, respectively. In addition, an independent-samples T test was performed to compare the latency and amplitude of components (P1, N170, and P2) according to the condition. The neural response data within groups were analyzed by one-way analysis of variance (ANOVA) according to the conditions. All neural data were tested for mean sum (Brown-Forsythe test) and homogeneity of variance (Tamhane's T2 test).

Source comparison analyses were performed on the basis of regionwise and timestepwise *t* tests, and the maximum adjacent timestep was set as 1. The critical value for a significance level of 5% was established by cluster-based permutation tests using 10,000 randomizations, similar to previous studies of Han et al.[33] and Sassenhagen et al.[34] Pearson's correlation analyses and linear regression analyses were used to analyze the associations in the neural data. $P < 0.05$ was considered statistically significant.

RESULTS

Participants

The data of 20 VD children, 20 TD children and 21 healthy adults were included in the final analyses. All participants were right-handed and grew up in a Mandarin-speaking environment. The mean ages were 6.48 ± 1.63 (5.2–9.6) years old in the VD group, 7.00 ± 1.29 (5.0–9.0) years old in the TD group, and 24.62 ± 2.71 (20.0–28.0) years old in the healthy adult group. The mean postoperative time in the VD group was 4.80 ± 1.25 (3.1–7.2) years. No significant differences in age ($P = 0.433$), sex ($P = 0.206$), or education ($P = 0.752$) were noted between the VD and TD groups. The binocular BCVAs were 0.24 ± 0.24 (0.01–0.7), 1.14 ± 0.09 (1.0–1.2), and 1.05 ± 0.03 (1.0–1.2) in the Snellen acuity of the VD, TD and healthy adult groups, respectively. There were significant differences regarding binocular BCVA ($P < 0.001$), oculus dexter BCVA ($P < 0.001$), and oculus sinister BCVA ($P < 0.001$) between the VD and TD groups.

ERPs

To identify VD deficits in visual processing, neural responses to visual stimuli in three groups (VD, TD and healthy adults) along the time course were investigated via ERPs. For each group, the amplitudes and latencies of the major components (P1, N170, and P2) in visual processing were separately extracted according to the peak ROI (O1, O2 in occipital areas, P7, P8 in temporal areas) and were compared among groups and conditions (Table).

Between-Group Comparisons of the Amplitudes and Latencies of ERPS

In this study, peak ROIs were chosen on a grand average head map collapsed from the averaged waveform of each group across all conditions and participants, to represent the peak location of each component. Then, the peak window was identified in the peak ROI waveform (for information on the identified peak ROI and peak time, see Supplementary Table S1). Based on these waveforms, peak amplitudes and latencies were extracted for further statistical tests. For the P1 component, which represents the primary visual processing after stimuli information is first projected from the retina to the visual cortex,[35,36] the VD group showed significantly lower P1 amplitudes than the TD group under all three conditions, but there was no difference in P1 latency occurred (see the representative P1 waveform in Figs. 2A and 2B and detailed results in Supplementary Table S1, full view of the waveform from all ROIs in Supplementary Fig. S3). To confirm that the differences in results were not caused by the BCVA divergences between the VD and TD groups, we conducted a correlation analysis between BCVA and P1 amplitudes. The results demonstrated that the BCVA level was not significantly correlated with the P1 amplitudes assessed at the peak ROI and time. For N170 and P2, no systematic difference was found between the VD and TD groups (see detailed results in Supplementary Table S1). In addition, the TD group showed generally greater amplitudes

TABLE. Significantly Different Task-Activated Regions Tested Along the Time Course

TD vs. VD	Character	Human Face	Object
Significant regions ($P < 0.05$)	Calcarine_R 100–144 ms Lingual_R 85–145 ms Lingual_R 279–344 ms Fusiform_R 87–126 ms	Calcarine_L 118–162 ms	Lingual_R 91–283 ms Fusiform_R 97–242 ms Temporal_Inf_R102–305 ms

All the significantly inhibited sources in VD children compared to TD children were found in relatively early stages (before 350 ms), mainly in the time range of P1 and N170 components.
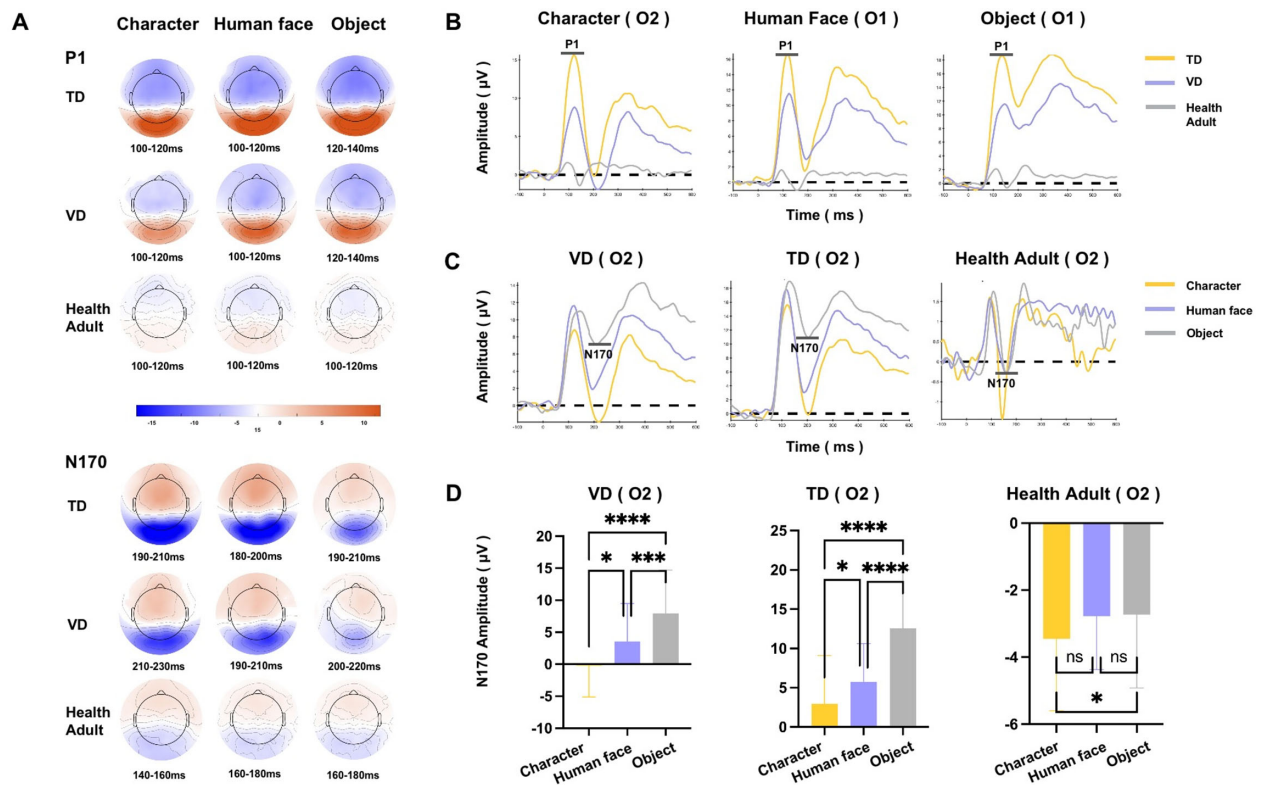
FIGURE 2. The ERP responses among groups and conditions. (**A**) The topography of ERPs. *Red* indicates positive activation, whereas *blue* indicates negative activation. (**B**) Between-group differences in the P1 waveform. The P1 amplitudes were lower in the VD group than in the TD group in the representative ROI of O1, which are shown as a representative region. (**C**) Between-condition differences in the N170 waveform in the representative ROI of O2. (**D**) Significant N170 effects in the peak ROI of three groups. The *asterisk* indicates a significant difference; *ns* indicates no significant difference. Both the VD and TD groups had obviously enhanced N170 for the character and face conditions. *$P < 0.05$; **$P < 0.01$; ***$P < 0.001$; ****$P < 0.0001$.

and longer latencies than healthy adults on P1, N170 and P2, revealing a normal developmental feature.

The ERP results revealed that the most significant difference in the early-stage visual processing of the VD group was the decreased P1 responses, which were situated in the visual cortices of V1 and V2 and the ventral-lateral occipital lobe of Brodmann areas 18 and 19,[37] which highlighted a deficit of restricted engagement during primary visual processing. However, the latencies of P1 showed no difference between the VD and TD groups, suggesting that temporal sensitivity was not obviously impaired or that projection timing was not delayed in the retinofugal pathway.

Between-Group Comparisons of the Condition Effects

The N170 component is sensitive to specific stimulus categories (e.g., human faces, Chinese characters), with larger N170 amplitudes in comparison to other stimuli. It represents the perceptual expertise effect in processing specific visual information, which is known as the 'N170 specialization effect'.[38–42] ANOVA tests of the N170 amplitudes were conducted on peak ROIs of N170 component in each group, and the results showed that, for both the VD and TD groups, there were strong N170 effects of characters and human faces in the peak ROI (O2) and time (ANOVA, character <object, human face <object, $P < 0.001$), suggesting that the VD group had no delay in discrimination sensitivity for complex visual stimuli. The healthy adults showed

enhanced N170 only under the character but not human face condition (ANOVA, character < object, $P < 0.05$), which may represent adults' proficiency in human face processing (Figs. 2C, 2D).

Task-Activated Source Activities

With a discrepancy among VD, TD and healthy adults found in the ERP data, we further probed task-activated source activity to reveal the source-level neural functional alterations in VD. The sensor density of up to 256 electrodes in this study enabled the possibility of high spatial resolution along the time courses of functional responses.

Cortico-cortical projections for visual processing that originate from the striate cortex are organized into two streams: the dorsal stream, known as the "Where-pathway," runs among the occipital lobes, the posterior parietal lobes, the premotor cortex and the frontal eye field; and the ventral stream, "What-pathway," projects from the occipital lobes to the inferior temporal region.[3,43] According to classic visual cortex and dorsal/ventral stream anatomy locations, we classified source-level activated regions into four main subnetworks: (1) visual cortex (lateral calcarine and occipital cortices); (2) ventral stream (lateral inferior temporal fusiform, lingual and parahippocampal); (3) dorsal stream (lateral middle temporal, medial superior temporal, posterior parietal, precuneus, frontal eye field and premotor areas); and (4) beyond network regions (all the other regions except the above three subnetworks).
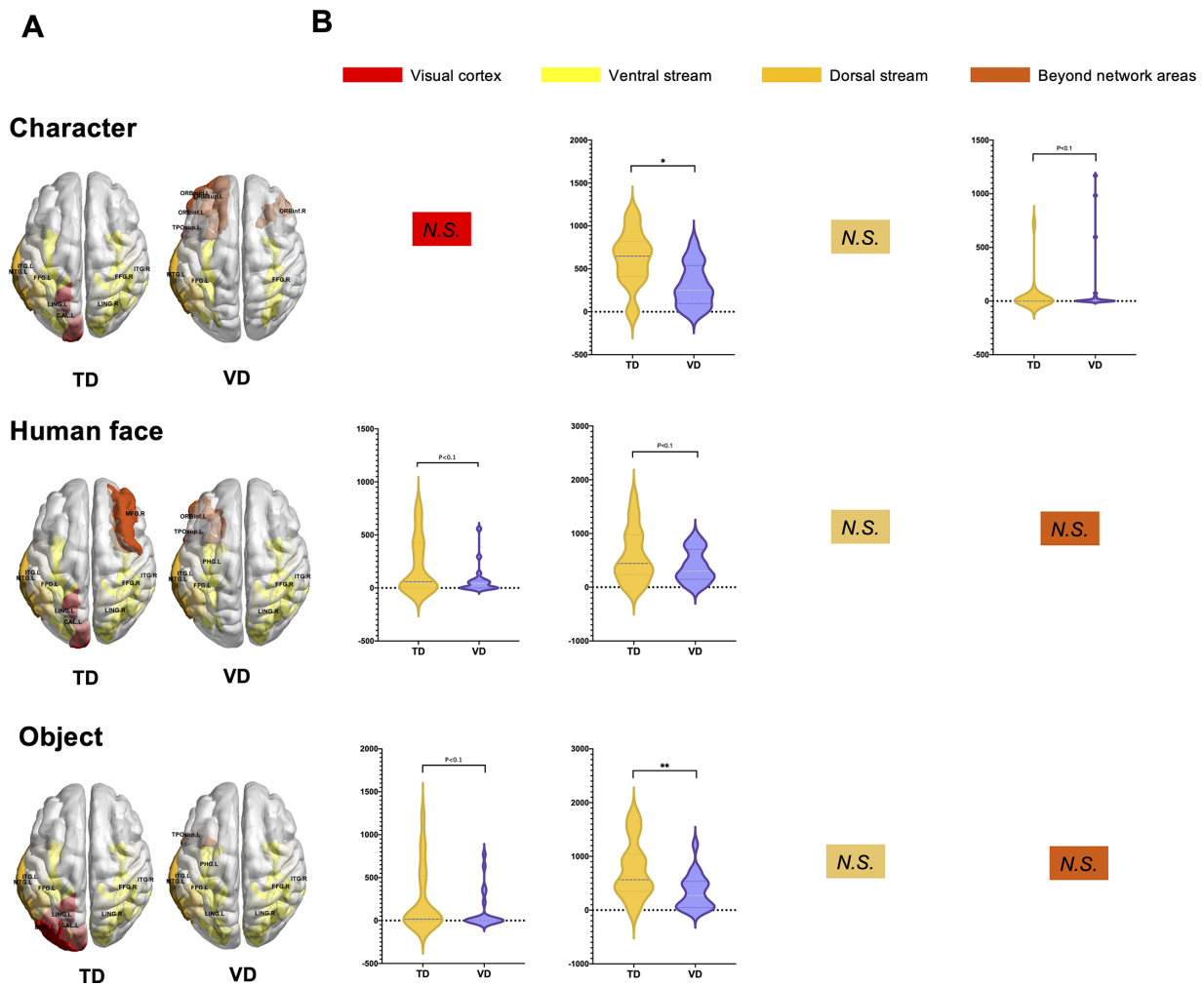
FIGURE 3. Functional region mapping of task activation. (**A**) Most activated regions during visual tasks for the TD and VD groups. The color of the regions indicates the type of subnetwork to which they belong. The VD group showed weak participation of the visual cortex, multiple inactive ventral stream areas mainly in the character and human face conditions, and hyperactive beyond-network regions. (**B**) Group comparisons of the activation of four subnetworks between the VD and TD groups (group level T test, $P < 0.05$). *$P < 0.05$; **$P < 0.01$; ***$P < 0.001$; ****$P < 0.0001$; N.S., Not significant ($P > 0.05$).

Functional Source Mapping

Highly activated cortical regions (top 10% of the activated regions) were identified in three conditions for the VD, TD and healthy adult groups, reflecting the functional source regions for visual tasks. The highly activated regions are visualized in Figure 3A, and details are listed in Supplementary Table S2.

Healthy Adults. Strong activation of the ventral/dorsal stream was found in healthy adults. Among all regions, the most activated regions were located in the ventral stream (including the bilateral lingual, fusiform, inferior temporal gyrus and parahippocampal regions) and dorsal stream subnetworks (including the left precuneus and right middle temporal gyrus). Consistent with our results, previous studies using similar tasks also suggested a vital function of the dorsal-ventral pathway.[44–48] Note that minor differences existed among the three conditions, with especially strong power in the left precuneus during the character and object conditions and special activation in the left parahippocampal during the face condition.

TD. Functional mapping in the TD children showed very similar ventral and dorsal stream participation that was very similar to that of healthy adults but with special activation enhancement in the visual cortex (calcarine and occipital middle gyrus) and a lack of intensive participation of the dorsal precuneus and ventral parahippocampal cortex.

VD. Three groups of idiosyncratic characteristics were found for the VD group compared with the TD group. First, inhibited activation in the visual cortex: neither primary nor higher level occipital regions were found in the highly activated regions, which was consistent with the decreased P1 amplitudes in the ERP analyses. Second, the attenuated ventral stream in the complex stimuli condition: multiple functional regions in the ventral stream were missing under the character and human face conditions, but the normal ventral stream area actively participated in the object condition. Interestingly, for the dorsal stream regions, VD children shared the same functional region of the middle temporal gyrus with TD children. Third, the hyperactive beyond-network regions: in VD, a range of regions beyond

the visual networks were found to intensively participate, especially in the character condition, and these regions were located mainly in frontal areas and the temporal pole.

Dynamic Functional Source Changes

A group comparison test was performed on task-activated source powers of 4 subnetworks to find significant differences between the VD and TD groups. As shown by the test results (visualized in Fig. 3B), the right ventral stream was found to show significantly lower activation in the VD group than in the TD group in both the character and object conditions (two-sided test, character condition: $P < 0.05$; object condition: $P < 0.01$). In addition, the visual cortex also showed decreased activation power in the VD group, but with marginal significance (two-sided test, face condition: $P < 0.1$; object condition: $P < 0.1$). On the other hand, only the right beyond subnetwork was found to indicate an enhanced source power level in VD children than in TD children (two-sided test, character condition: $P < 0.1$).

Alpha Band Oscillations at the Source Level

With the whole-brain source activation well probed, we further analyzed the alpha band oscillatory features of each subnetwork both prior to and after stimuli presentation. Alpha band power has been widely recognized to be linked to the alerting system of attention, which is crucial for visual perception. Alpha oscillatory activity is the only frequency band that shows a decrease in power during visual stimulation and an increase in power in the absence of visual input[49,50]; hence, the post-stimulus alpha PSD has been linked to the integration of the top-down attentional process. In addition, early studies showed that alpha power decreased when a visual target was anticipated,[51,52] supporting the notion that pre-stimulus alpha band activity was related to the alerting system of attention.[53] To the best of our knowledge, no previous study has directly investigated alpha oscillations on source-level task-state neural activities.

Pre-Stimulus Alpha PSD

For alpha band activity during the −500 ms to 0 ms before the stimuli, beyond network areas were found to show
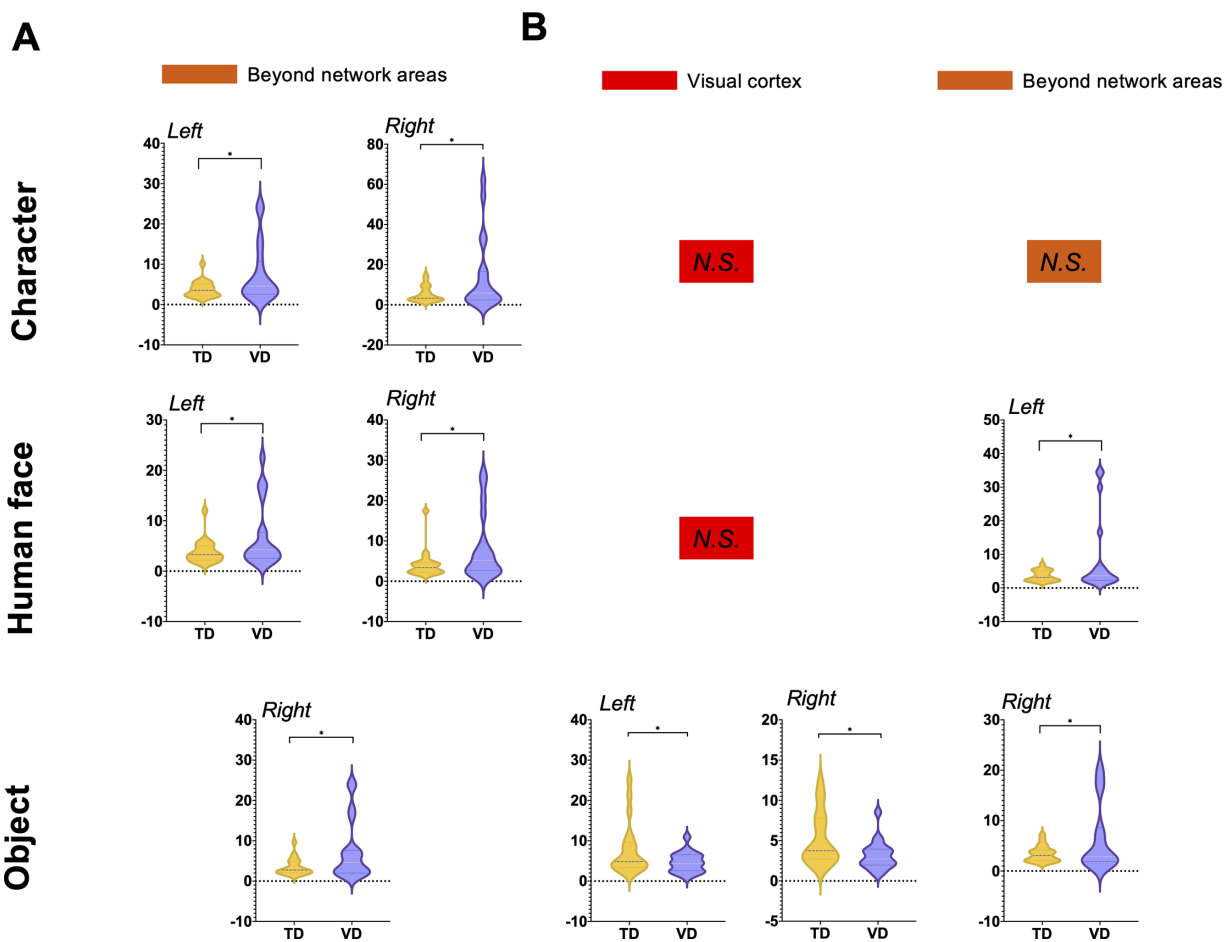

FIGURE 4. Pre-stimulus and post-stimulus alpha band PSD. In the analysis of the alpha band PSD of each subnetwork between the VD and TD groups in the comparison test, all significant subnetworks are visualized in this figure (T test, $P_{FDR} < 0.05$). The violin graphs illustrate the alpha power of the VD and TD groups in each subnetwork. The VD group showed generally enhanced pre-stimulus alpha PSD in all three conditions in beyond network areas. The VD group showed decreased post-stimulus alpha PSD in the visual cortex but enhanced post-stimulus PSD in beyond network areas. *$P < 0.05$; **$P < 0.01$; ***$P < 0.001$; ****$P < 0.0001$; N.S., Not significant ($P > 0.05$).

significantly different PSD between the VD group and the TD group in the region-wise group comparison test (*t* test, P_{FDR} < 0.05). Specifically, enhanced alpha-band PSD was found in beyond network areas, under all three conditions, as visualized in Figure 4 (detailed results provided in Supplementary Table S3). The enhanced prestimulus alpha band activity may indicate a disengaged cortical state of the top-down mediation and attentional participation in the VD group.

Post-Stimulus Alpha PSD

For alpha band PSD during 0–500 ms after the stimuli, a clear divergence from the visual cortex and beyond network areas was revealed in the group comparison results (visualized in Fig. 4 and details listed in Supplementary Table S4). For the visual cortex, the VD group showed significantly lower alpha band PSD than the TD group (*t* test, P_{FDR} < 0.05). However, the beyond network areas were also found to be significant, yet the VD group showed larger post-stimulus alpha PSD than the TD group (*t* test, P_{FDR} < 0.05). The enhanced alpha oscillation indicated a deficit of the top-down attentional process in the frontal regions, but the inhibited alpha PSD in visual cortex areas might suggest increased task engagement of primary visual regions.

Discussion

Neural Functional Impairment of Children With Innate Binocular VD

Underdeveloped Primary Visual Cortex and Ventral Stream. One of the most significant insights of the current study is pinpointing the associations between impaired visual function of VD children and the underdeveloped primary visual cortex as well as inhibited ventral stream, which served as proof of and support for the hypothesis of the abnormal development of the visual functional area of the cerebral cortex caused by early binocular VD.[54] On the scalp-level EEG data, the amplitudes of early ERP component P1 evoked by the visual processing tasks were generally decreased in the VD group compared with the TD controls under all three conditions, which indicated a deficit in primary visual processing. Occipitotemporal P1 is an obligatory and exogenous sensory response to visual stimuli, involving an attention effect that reflects a general-purpose visual discrimination mechanism.[55,56] The inhibited P1 amplitude results concurred with the findings in task-activated sources, pinned to early-stage processing.

Successful vision relies on the integrity of the pathway between the retina and the primary visual cortex.[1,3] Anatomical studies on the neurodevelopmental mechanisms in the human visual system have found that high-quality visual input plays a critical role in the early-stage development of the V1 cortex and a rapid increase in the number of dendrites and synaptic connections in the striate cortex during the first months after birth, which peaks between 8 months and 2 years of life.[57,58] Our findings indicated that VD at a very early age caused impairment and delay in the function of the primary visual cortex and might explain poor visual recovery after successful treatment in VD children.

All the VD participants enrolled in our study had relatively normal ocular structure and electrooculogram results, but their BCVAs were lower than clinically expected, which is common in post-therapeutic childhood patients with innate oculopathies.[59–61] These children are recommended to have amblyopia training to benefit visual recovery; however, the effects are sometimes unsatisfactory.[62,63] According to the results, the vision conduction speed from the retina to the primary visual cortex was similar between the VD and TD groups, as the P1 latencies showed no significant between-group difference. Nevertheless, the underdeveloped primary visual cortex generated impaired visual information processing, which was potentially an important reason for low BCVAs and slow recovery of visual function.

In addition, the visual function deficit was further traced to the reduced source-level activities of the visual cortex and ventral stream subnetworks. Specifically, the ventral stream is one of the dual streams of visual processing that have been well recognized by lesion and neuroimaging studies: the dorsal stream areas are mainly involved in functions such as spatial cognition, spatial attention, motion perception, visuomotor integration, grasping coordination, egocentric body representation, or mental rotation, whereas the ventral stream supports high-order visual functions, such as object recognition, visual memory, semantic retrieval or complex symbol recognition.[64–68] Because the discrimination of E orientation in E-chart examination highly depends on the effective functioning of the ventral stream, the deficits of the ventral stream in VD children can explain their poor function in visual recognition and poor performance in the E-chart examination. In addition, we speculate that the application of symbol charts for visual tests may be more suitable for the VD group,[69,70] which mainly depends on the dorsal stream during recognition and perhaps can provide more information on VA changes.

Impaired Top-Down Attention During Visual Processing. In addition to the deficits in the visual cortex and ventral stream, impaired top-down attention during visual processing in VD children was also found based on increased pre-stimulus alpha oscillation compared to that of TD children. A great number of previous works have suggested that alpha band activity may be linked to the integration of top-down and bottom-up attentional processes, where alpha synchronization/enhancement is associated with activated inhibition of information flow and reduced task engagement, and alpha inhibition is related to facilitation of information flow and increased task engagement, such as release from inhibition.[71]

In this study, beyond network regions (mostly frontal and temporal pole areas) of the VD children were found to have increased pre-stimulus alpha oscillations, suggesting relatively disengaged top-down attentional engagement compared to that in TD children. The orbitofrontal cortex plays a critical role in visuo-affective prediction by facilitating recognition of sensory inputs via predictive feedback to sensory cortices,[72,73] while the temporal pole is crucial in a range of high-level visual functions,[74] as well as in receiving perceptual inputs from multiple sensory streams, including the ventral visual stream and the integration of emotion with perception.[75] These findings indicate that an impaired top-down alerting system and high-level association during visual processing may lead to low visual function and sensitivity in VA examinations of the VD group. Based on the defects in top-down attention, the effects of traditional visual training are limited. We propose that a more beneficial method composed of an attentional alerting system and vision tasks probably contributes to the success of visual recognition. Several training programs have been proposed to improve executive attention in several groups with different mental disabilities and have been proven

effective in top-down attention improvement,[76–78] whereas their availability for children with innate visual impairment needs further clinical invalidation.

Plasticity Potentials for Compensational Visual Function Development

Visual Discrimination Sensitivity and Increased Bottom-Up Visual Attention. Despite the deficits and impairments of neural functions found in VD visual processing, the findings involving discrepancies in responses for different types of visual tasks shed light on the plasticity potential of the VD group. The occipitotemporal negative N170 component was recognized as an important visual perception component that was strongly elicited by certain classes of visual stimuli, such as faces and words, which were hypothesized to demonstrate perceptual expertise effects.[79,80] The character- and face- specific N170 effect, as an important signature of visual discrimination development, was found in both the VD and TD groups, suggesting intact discrimination sensitivity in the VD group. Such sensitivity may offer a foundation for learning the most important complex symbol system, written words, which is crucial for school study. The lack of an N170 effect of face condition in adults may be due to facial expression and face size, which is consistent with previous studies.[81–83] Based on the results, VD children have the potential to obtain the ability of written word recognition as the TD group. However, the training of word reading after surgery is rarely mentioned or paid attention to by researchers, which needs further exploration considering the importance of reading ability and its crucial part in study.

The inhibited alpha PSD in visual cortex areas indicated that VD strengthened the bottom-up attentional process in the object condition. For alpha band PSD during 0-500 ms after stimuli, distinctiveness for the object condition was revealed. Compared to complex stimuli (character and human face), the subnetwork of the visual cortex was found to have decreased alpha-band activity (also known as alpha desynchronization) in the object condition, suggesting enhanced bottom-up attention with increased task engagement that facilitated visual information flow and played a compensatory role. To improve the less-developed function of the visual cortex, object recognition training is probably a good choice to activate its potential for recovery. The figures of daily objects can probably be adopted as training materials for ventral stream activation and visual recovery. In addition, a wide range of studies have revealed that noninvasive transcranial electrical/magnetic stimulation of the functional cortices could improve the recovery of motoric, language and cognitive functions in patients with stroke and other neural impairments.[84–86] Such methods, however, are rarely adopted during visual rehabilitation after the removal of the cause of VD. Our findings have shed light on possible stimulation areas that could be simulated, such as beyond network regions, which may provide a more practical method to promote visual recovery after the cause of innate binocular VD has been removed.

Well-Functioning Dorsal Stream Activity. In contrast, with the impairment of the ventral stream, the dorsal stream remained unaltered in VD children, with no significant difference in dorsal stream areas in either source region activation or alpha oscillation found between the groups. The well-functioning dorsal stream activity in VD may result from the importance of location and motion information for daily life living and safety. Previous studies have also proposed that infants learn about objects through tactile handling; therefore, knowing how to handle objects and observe them (through the dorsal stream) must be developed before the ventral stream processes what the object represents.[87] Given the functional impairment found in the ventral stream, obvious asymmetry was identified in the visual processing network of VD children. Similarly, asymmetry between the ventral and dorsal streams has also been found in a brain structural study on congenital blindness, in which reduced fractional anisotropy in the ventral stream but not in the dorsal stream was found. This is possibly caused by the asymmetry of functional reliance by VD, because spatial cognition is more vital for them to survive (e.g., recognizing the presence of obstacles and walking safely). This observation enhances the understanding of the interactive relations between the ventral and dorsal streams in early development.

Assessing dynamic neural function in whole-brain visual networks is challenging in terms of technique. Technical and methodological limitations may have restricted the conduction of related research. Some published studies have defined the neurological changes in bilaterally blind children and adults using functional magnetic resonance imaging (MRI),[88,89] which lacks high-temporal resolution or rest-state data that negatively affect the characterization of dynamic neural processing in real time.[90] Fortunately, the application of HD-EEG improves the research dilemma with the advantages of noninvasive, nonradiant, real-time and less-discomfort features.[91–93] In addition, HD-EEG localized significantly closer to the anatomical reference point obtained by functional MRI in the source analysis, which further proves the spatial positioning accuracy of HD-EEG.[94]

Limitations

Some limitations need to be considered. First, the number of VD children investigated in this study was limited; increased participant sample sizes, as well as participants from other centers, are necessary to strengthen our results. In addition, neural functional changes before and after treatment in VD children can help understand the effect of visual loss on cerebral development after birth. Moreover, more studies of other congenital oculopathies and their neural characteristics need to be conducted to generalize our findings. Despite the activation deficit, the ERP analyses also showed a normal latency of P1 and other critical components in the VD group compared with the TD children, possibly suggesting intact optic radiation. Although the development of optic radiation is not fully probed in the current study, this finding leaves an interesting issue for interpretation and further investigation.

CONCLUSION

Using HD-EEG and state-of-the-art analysis, in the present study we examined neural responses to varying visual stimuli in children after the cause of innate binocular VD was removed and characterized the functional deficits, as well as compensatory mechanisms in brain regions. Binocular VD at early ages caused an underdeveloped primary visual cortex, inhibition in the ventral stream and impaired top-down attention. Compensatory neural activities were identified in bottom-up visual attention and the dorsal stream.

For the first time, dynamic visual neural activities in the task state were investigated across whole-brain networks, which contributed to a better understanding of visual processing after VD and shed light on more appropriate visual training strategies.

References

1. Felleman DJ, Van Essen DC. Distributed Hierarchical Processing in the Primate Cerebral Cortex. *Cerebral Cortex*. 1991;1:1–47.
2. Goodale MA, Milner AD. Separate visual pathways for perception and action. *Trends Neurosci*. 1992;15:20–25.
3. Ungerleider LG, Mishkin M. Two cortical visual systems. *Anal Vis Behav*. 1982;549:chapter 18.
4. Diao Y, Chen Y, Zhang P, Cui L, Zhang J. Molecular guidance cues in the development of visual pathway. *Protein Cell*. 2018;9:909–929.
5. Cheung S-H, Fang F, He S, Legge GE. Retinotopically Specific Reorganization of Visual Cortex for Tactile Pattern Recognition. *Curr Biol*. 2009;19:596–601.
6. Sadato N, Pascual-Leone A, Grafman J, Deiber MP, Ibañez V, Hallett M. Neural networks for Braille reading by the blind. *Brain*. 1998;121:1213–1229.
7. Wittenberg G, Werhahn K, Wassermann E, Herscovitch P, Cohen L. Functional connectivity between somatosensory and visual cortex in early blind humans. *Eur J Neurosci*. 2004;20:1923–1927.
8. Jain IS, Pillai P, Gangwar DN, Gopal L, Dhir SP. Congenital cataract: management and results. *J Pediatr Ophthalmol Strabismus*. 1983;20:243–246.
9. Russell HC, McDougall V, Dutton GN. Congenital cataract. *BMJ*. 2011;342:d3075.
10. Pascolini D, Mariotti SP. Global estimates of visual impairment: 2010. *Br J Ophthalmol*. 2012;96:614–618.
11. Constantinescu T, Schmidt L, Watson R, Hess RF. A residual deficit for global motion processing after acuity recovery in deprivation amblyopia. *Invest Ophthalmol Vis Sci*. 2005;46:3008–3012.
12. Ellemberg D, Lewis TL, Maurer D, Brar S, Brent HP. Better perception of global motion after monocular than after binocular deprivation. *Vis Res*. 2002;42:169–179.
13. Jeffrey BG, Wang YZ, Birch EE. Altered global shape discrimination in deprivation amblyopia. *Vis Res*. 2004;44:167–177.
14. Lewis TL, Ellemberg D, Maurer D, et al. Sensitivity to global form in glass patterns after early visual deprivation in humans. *Vis Res*. 2002;42:939–948.
15. Geldart S, Mondloch CJ, Maurer D, De Schonen S, Brent HP. The effect of early visual deprivation on the development of face processing. *Dev Sci*. 2002;5:490–501.
16. Le Grand R, Mondloch CJ, Maurer D, Brent HP. Impairment in holistic face processing following early visual deprivation. *Psychol Sci*. 2004;15:762–768.
17. Kupers R, Ptito M. Compensatory plasticity and cross-modal reorganization following early visual deprivation. *Neurosci Biobehav Rev*. 2014;41:36–52.
18. Ptito M, Matteau I, Zhi Wang A, Paulson OB, Siebner HR, Kupers R. Cross-modal recruitment of the ventral visual stream in congenital blindness. *Neural Plast*. 2012;2012:304045.
19. Atkinson J. *The Developing Visual Brain*. Oxford: Oxford University Press; 2002.
20. Bentin S, Deouell LY, Soroker N. Selective visual streaming in face recognition: evidence from developmental prosopagnosia. *Neuroreport*. 1999;10:823–827.
21. Itier R, Taylor M. N170 or N1? Spatiotemporal differences between object and face processing using ERPs. *Cereb Cortex*. 2004;14:132–142.
22. Maurer D, Lewis TL, Mondloch CJ. Missing sights: consequences for visual cognitive development. *Trends Cogn Sci*. 2005;9:144–151.
23. Maurer U, Brem S, Bucher K, et al. Impaired tuning of a fast occipito-temporal response for print in dyslexic children learning to read. *Brain*. 2007;130:3200–3210.
24. Maurer U, Brem S, Kranz F, et al. Coarse neural tuning for print peaks when children learn to read. *NeuroImage*. 2006;33:749–758.
25. Luck SJ. *An introduction to the event-related potential technique*. Cambridge, MA: MIT Press; 2014.
26. Pascual-Marqui RD. Standardized low-resolution brain electromagnetic tomography (sLORETA): technical details. *Methods Find Exp Clin Pharmacol*. 2002;24(Suppl D):5–12.
27. Luu P, Tucker DM, Stripling R. Neural mechanisms for learning actions in context. *Brain Res*. 2007;1179:89–105.
28. Tzourio-Mazoyer N, Landeau B, Papathanassiou D, et al. Automated anatomical labeling of activations in SPM using a macroscopic anatomical parcellation of the MNI MRI single-subject brain. *Neuroimage*. 2002;15:273–289.
29. Coito A, Plomp G, Genetti M, et al. Dynamic directed interictal connectivity in left and right temporal lobe epilepsy. *Epilepsia*. 2016;57:1351.
30. Hatlestad-Hall C, Bruña R, Syvertsen MR, et al. Source-level EEG and graph theory reveal widespread functional network alterations in focal epilepsy. *Clin Neurophysiol*. 2021;132:1663–1676.
31. Urriola J, Bollmann S, Tremayne F, Burianová H, Marstaller L, Reutens D. Functional connectivity of the irritative zone identified by electrical source imaging, and EEG-correlated fMRI analyses. *Neuroimage Clin*. 2020;28:102440.
32. Xia M, Wang J, He Y. BrainNet Viewer: a network visualization tool for human brain connectomics. *PLoS ONE*. 2013;8:e68910.
33. Han CE, Yoo SW, Seo SW, Na DL, Seong JK. Cluster-based statistics for brain connectivity in correlation with behavioral measures. *PLoS One*. 2013;8(8):e72332.
34. Sassenhagen J, Blything R, Lieven EVM, Ambridge B. Frequency sensitivity of neural responses to English verb argument structure violations. *Collabra Psychol*. 2018; 4:38.
35. Gomez Gonzalez CM, Clark VP, Fan S, Luck SJ, Hillyard SA. Sources of attention-sensitive visual event-related potentials. *Brain Topogr*. 1994;7:41–51.
36. Woldorff MG, Fox PT, Matzke M, et al. Retinotopic organization of early visual spatial attention effects as revealed by PET and ERPs. *Hum Brain Mapp*. 1997;5:280–286.

37. Clark VP, Hillyard SA. Spatial selective attention affects early extrastriate but not striate components of the visual evoked potential. *J Cogn Neurosci*. 1996;8:387–402.

38. Amihai I, Deouell LY, Bentin S. Neural adaptation is related to face repetition irrespective of identity: a reappraisal of the N170 effect. *Exp Brain Res*. 2011;209:193–204.

39. Eimer M, Kiss M, Nicholas S. Response profile of the face-sensitive N170 component: a rapid adaptation study. *Cereb Cortex*. 2010;20:2442–2452.

40. Fu S, Feng C, Guo S, Luo Y, Parasuraman R. Neural adaptation provides evidence for categorical differences in processing of faces and Chinese characters: an ERP Study of the N170. *PloS one*. 2012;7:e41103.

41. Harris A, Nakayama K. Rapid face-selective adaptation of an early extrastriate component in MEG. *Cereb Cortex*. 2007;17:63–70.

42. Harris A, Nakayama K. Rapid adaptation of the M170 response: importance of face parts. *Cereb Cortex*. 2008;18:467–476.

43. Tong F. Primary visual cortex and visual awareness. *Nat Rev Neurosci*. 2003;4:219–229.

44. Horovitz SG, Rossion B, Skudlarski P, Gore JC. Parametric design and correlational analyses help integrating fMRI and electrophysiological data during face processing. *Neuroimage*. 2004;22:1587–1595.

45. Itier RJ, Taylor MJ. Source analysis of the N170 to faces and objects. *Neuroreport*. 2004;15:1261–1265.

46. Nobre AC, Allison T, McCarthy G. Word recognition in the human inferior temporal lobe. *Nature*. 1994;372:260–263.

47. Schweinberger SR, Pickering EC, Jentzsch I, Burton AM, Kaufmann JM. Event-related brain potential evidence for a response of inferior temporal cortex to familiar face repetitions. *Cogn Brain Res*. 2002;14:398–409.

48. Kanwisher N, McDermott J, Chun MM. The fusiform face area: a module in human extrastriate cortex specialized for face perception. *J Neurosci*. 1997;17:4302.

49. Klimesch W. EEG alpha and theta oscillations reflect cognitive and memory performance: a review and analysis. *Brain Res Brain Res Rev*. 1999;29:169–195.

50. Klimesch W. α-Band oscillations, attention, and controlled access to stored information. *Trends Cogn Sci*. 2012;16:606–617.

51. Foxe JJ, Simpson GV, Ahlfors SP. Parieto-occipital approximately 10 Hz activity reflects anticipatory state of visual attention mechanisms. *Neuroreport*. 1998;9:3929–3933.

52. Klimesch W, Doppelmayr M, Russegger H, Pachinger T, Schwaiger J. Induced alpha band power changes in the human EEG and attention. *Neurosci Lett*. 1998;244:73–76.

53. Fan J, Byrne J, Worden MS, et al. The relation of brain oscillations to attentional networks. *J Neurosci*. 2007;27:6197–6206.

54. Wright KW, Matsumoto E, Edelman PM. Binocular fusion and stereopsis associated with early surgery for monocular congenital cataracts. *Arch Ophthalmol*. 1992;110:1607–1609.

55. Luck S, Kappenman E. ERP Components and Selective Attention. In: *The Oxford handbook of event-related potential components*. Oxford, UK: Oxford University Press; 2012;295–328.

56. Vogel E, Luck S. The visual N1 component as an index of a discrimination process. *Psychophysiology*. 2000;37:190–203.

57. Huttenlocher PR, Courten CD. The development of synapses in striate cortex of man. *Hum Neurobiol*. 1987;6:1–9.

58. Huttenlocher PR, De C, Garey LJ, Van D. Synaptic development in human cerebral cortex. *Int J Neurol*. 1982;16-17:144.

59. Chia W-LA, Martin F. Childhood cataracts. *Clin Exp Ophthalmol*. 2001;29:75–80.

60. deLuise VP, Anderson DR. Primary infantile glaucoma (congenital glaucoma). *Surv Ophthalmol*. 1983;28:1–19.

61. Morken TS, Dammann O, Skranes J, Austeng D. Retinopathy of prematurity, visual and neurodevelopmental outcome, and imaging of the central nervous system. *Semin Perinatol*. 2019;43:381–389.

62. Levi DM, Knill DC, Bavelier D. Stereopsis and amblyopia: A mini-review. *Vis Res*. 2015;114:17–30.

63. Wang M, Xiao W. Congenital cataract: progress in surgical treatment and postoperative recovery of visual function. *Eye Sci*. 2015;30:38–47.

64. Creem S, Proffitt D. Defining the cortical visual systems: "what", "where", and "how." *Acta Psychol*. 2001;107:43–68.

65. Grill-Spector K, Knouf N, Kanwisher N. The fusiform face area subserves face perception, not generic within-category identification. *Nat Neurosci*. 2004;7:555–562.

66. Milner AD, Goodale MA. *The Visual Brain In Action*. Oxford, UK: Oxford University Press; 1995.

67. Ungerleider LG, Haxby JV. "What" and "where" in the human brain. *Curr Opin Neurobiol*. 1994;4:157–165.

68. Atkinson J. *The Developing Visual Brain*. Oxford, UK: Oxford University Press; 2002.

69. Vivekanand U, Gonsalves S, Bhat SS. Is LEA symbol better compared to Snellen chart for visual acuity assessment in preschool children? *Rom J Ophthalmol*. 2019;63:35–37.

70. Hyvärinen L, Näsänen R, Laurinen P. New visual acuity test for pre-school children. *Acta Ophthalmol*. 1980;58:507–511.

71. Klimesch W. Alpha-band oscillations, attention, and controlled access to stored information. *Trends Cogn Sci*. 2012;16:606–617.

72. Chaumon M, Kveraga K, Barrett LF, Bar M. Visual predictions in the orbitofrontal cortex rely on associative content. *Cereb Cortex*. 2013;24:2899–2907.

73. Liu D, Deng J, Zhang Z, et al. Orbitofrontal control of visual cortex gain promotes visual associative learning. *Nat Commun*. 2020;11:2784.

74. Herlin B, Navarro V, Dupont S. The temporal pole: from anatomy to function—a literature appraisal. *J Chem Neuroanat*. 2021;113:101925.

75. Olson IR, Plotzker A, Ezzyat Y. The enigmatic temporal pole: a review of findings on social and emotional processing. *Brain*. 2007;130:1718–1731.

76. de Greeff JW, Bosker RJ, Oosterlaan J, Visscher C, Hartman E. Effects of physical activity on executive functions, attention and academic performance in preadolescent children: a meta-analysis. *J Sci Med Sport*. 2018;21:501–507.

77. Halperin JM, Marks DJ, Chacko A, et al. Training Executive, Attention, and Motor Skills (TEAMS): a preliminary randomized clinical trial of preschool youth with ADHD. *J Abnorm Child Psychol*. 2020;48:375–389.

78. McKay E, Richmond S, Kirk H, Anderson V, Catroppa C, Cornish K. Training attention in children with acquired brain injury: a study protocol of a randomised controlled trial of the TALI attention training programme. *BMJ Open*. 2019;9:e032619.

79. Joyce C, Rossion B. The face-sensitive N170 and VPP components manifest the same brain processes: the effect of reference electrode site. *Clin Neurophysiol*. 2005;116:2613–2631.

80. Rossion B, Joyce CA, Cottrell GW, Tarr MJ. Early lateralization and orientation tuning for face, word, and object processing in the visual cortex. *Neuroimage*. 2003;20:1609–1624.

81. Schweinberger SR, Huddy V, Burton AM. N250r: a face-selective brain response to stimulus repetitions. *Neuroreport*. 2004;15:1501–1505.

82. Schweinberger SR, Kaufmann JM, Moratti S, Keil A, Burton AM. Brain responses to repetitions of human and animal

faces, inverted faces, and objects: an MEG study. *Brain Res*. 2007;1184:226–233.

83. Thierry G, Martin CD, Downing P, Pegna AJ. Controlling for interstimulus perceptual variance abolishes N170 face selectivity. *Nat Neurosci*. 2007;10:505–511.

84. Paik N, Celnik P, Cohen L. Effects of combined peripheral nerve stimulation and noninvasive anodal cortical stimulation on motor learning in chronic stroke. *Arch Phys Med Rehabil*. 2006;87:e2.

85. Blesneag AV, Popa L, Stan AD. Non-invasive brain stimulation in early rehabilitation after stroke. *J Med Life*. 2015;8(Spec Issue):52–56.

86. Kapoor A. Repetitive transcranial magnetic stimulation therapy for post-stroke non-fluent aphasia: A critical review. *Top Stroke Rehabil*. 2017;24:547–553.

87. Johnson MH, Munakata Y. Processes of change in brain and cognitive development. *Trends Cogn Sci*. 2005;9:152–158.

88. Grady CL, Mondloch CJ, Lewis TL, Maurer D. Early visual deprivation from congenital cataracts disrupts activity and functional connectivity in the face network. *Neuropsychologia*. 2014;57:122–139.

89. Maurer D, Mondloch CJ, Lewis TL. Effects of early visual deprivation on perceptual and cognitive development. *Prog Brain Res*. 2007;164:87–104.

90. Cargnelutti E, Ius T, Skrap M, Tomasino B. What do we know about pre- and postoperative plasticity in patients with glioma? A review of neuroimaging and intraoperative mapping studies. *Neuroimage Clin*. 2020;28:102435.

91. Zou Y, Lui M, Tsang YK. The roles of lexical tone and rime during Mandarin sentence comprehension: an event-related potential study. *Neuropsychologia*. 2020;147:107578.

92. Mheich A, Dufor O, Yassine S, et al. HD-EEG for tracking sub-second brain dynamics during cognitive tasks. *Sci Data*. 2021;8:32.

93. Comolatti R, Pigorini A, Casarotto S, et al. A fast and general method to empirically estimate the complexity of brain responses to transcranial and intracranial stimulations. *Brain Stimul*. 2019;12:1280–1289.

94. Klamer S, Elshahabi A, Lerche H, et al. Differences Between MEG and High-Density EEG Source Localizations Using a Distributed Source Model in Comparison to fMRI. *Brain Topogr*. 2015;28:87–94.